Applied Surface Science 256 (2010) 5011–5014

Contents lists available at ScienceDirect

Applied Surface Science

journal homepage: www.elsevier.com/locate/apsusc

Roughness evolution of Si surfaces upon Ar ion erosion

V.I.T.A. de Rooij-Lohmann[a,*], I.V. Kozhevnikov[b], L. Peverini[c], E. Ziegler[c], R. Cuerno[d], F. Bijkerk[a,e], A.E. Yakshin[a]

[a] FOM Institute for Plasma Physics Rijnhuizen, Postbus 1207, 3430 BE Nieuwegein, The Netherlands
[b] Institute of Crystallography, Leninsky prospect 59, Moscow 119333, Russia
[c] European Synchrotron Radiation Facility, BP 220, 38043 Grenoble Cedex, France
[d] Universidad Carlos III Madrid, GISC, E-28911 Leganes, Spain
[e] MESA+ Institute for Nanotechnology, University of Twente, Postbus 217, 7500 AE Enschede, The Netherlands

ARTICLE INFO

Article history:
Received 23 December 2009
Accepted 4 March 2010
Available online 15 March 2010

Keywords:
X-ray scattering
Ion erosion
Dynamic scaling
Si

ABSTRACT

We studied the roughness evolution of Si surfaces upon Ar ion erosion in real time. Following the theory of surface kinetic roughening, a model proposed by Majaniemi was used to obtain the value of the dynamic scaling exponent β from our data. The model was found to explain both the observed roughening and the smoothening of the surfaces. The values of the scaling exponents α and β, important for establishing a universal model for ion erosion of (Si) surfaces, have been determined. The value of β proved to increase with decreasing ion energy, while the static scaling exponent α was found to be ion energy independent.

1. Introduction

The analysis of Si surface roughness evolution under ion treatment and the determination of technological parameters necessary to preserve or to improve the surface smoothness are becoming increasingly important for advanced, reflective X-ray/Extreme Ultraviolet (EUV) optics. This notably concerns the next generation of optics [1], where ion etching is used to figure a macroscopic Si substrate with sub-nanometer accuracy while the microscopic roughness is maintained at an atomic level [2]. It is furthermore of major importance for the fabrication of multilayer reflective coatings for EUV optics, because the reflectivity of Mo/Si multilayer mirrors is influenced by the ion polishing steps in the manufacturing process [3–5].

In general, a variety of surface patterns can be observed upon ion treatment (smoothening, roughening, formation of ripples, nanodots, etc.), see, e.g., Ref. [6]. These topographies depend on the etch time, the surface material, the ion energy, and the ion angle of incidence. The final surface topography is determined by competing roughening and smoothening mechanisms with different spatial frequency and time dependencies. A surface that is growing or eroding under non-equilibrium conditions often develops as a fractal-like structure. This effect has been observed and formalized within the theoretical framework of surface dynamic scaling or kinetic roughening [7,8]. In this concept, several parameters, known as scaling exponents, can be used as the signatures in space and time of the growth or etch processes. By comparing the experimental scaling exponent values with the theoretical predictions, one can establish, in principle, a differential equation describing the film growth or erosion at a mesoscopic level. As an example, it was demonstrated in [9] that the evolution of the roughness of a tungsten film during Ar^+ ion erosion is consistent with the prediction of the Kardar–Parisi–Zhang (KPZ) equation [7]. Being a universal description of the ion erosion of Si surfaces, such an equation would contribute tremendously to the understanding of the interplay between the mechanisms leading to different morphologies and dynamics for ion-eroded surfaces [10], and also provide the ultimate tool for the selection of etch settings that lead to the best smoothening results.

The classical formulation of the scaling model assumes that the initial substrate is perfectly smooth. A number of questions arise in this framework. For instance, how does a non-zero roughness of the initial substrate affect the scaling model? Does the scaling behaviour depend on the initial substrate roughness? Is it possible to divide the eroded surface roughness into contributions from the initial substrate roughness and from the erosion induced roughness, the latter following the scaling law? The scaling concept is usually used to describe roughening, but can it also describe smoothening of a surface? Answers to these questions are important for the further development of the ion etching technology.

* Corresponding author. Tel.: +31 030 6096 874; fax: +31 030 6031 204.
E-mail addresses: V.I.T.A.deRooij@rijnhuizen.nl, veroniquederooij@gmail.com (V.I.T.A. de Rooij-Lohmann).
URL: http://www.rijnhuizen.nl (V.I.T.A. de Rooij-Lohmann).

0169-4332/$ – see front matter © 2010 Elsevier B.V. All rights reserved.
doi:10.1016/j.apsusc.2010.03.045

In the present paper we describe experimental results on a study of the surface evolution of Si substrates with a different initial roughness upon Ar ion treatment. The goals of the study are (a) verification of the scaling model at the initial stage of ion etching, when the initial substrate roughness gives an essential contribution to that of an eroded surface, (b) analysis of the dependency of the surface dynamics on the initial substrate roughness and the ion energy, and (c) analysis of the possibility to distinguish between the two factors that contribute to the roughness of an eroding surface, viz. the initial surface roughness and the erosion induced roughness.

2. Materials and methods

Among different techniques used for determination of the scaling parameters, the X-ray Scattering (XRS) method has a number of advantages, like allowing to study the evolution of the surface roughness in situ and in real time. This is essential, because oxidation or contamination by a vacuum background may result in an uncontrolled development of the surface roughness.

The experiments have been conducted at the grazing incidence X-ray reflectometry setup at the BM5 beamline of the ESRF synchrotron facility. The setup has been described in detail in, e.g., Ref. [11]. B-doped (1 0 0) silicon wafers with a thickness of 725 μm were used as substrates and mounted in a vacuum chamber. The X-ray beam enters and exits the chamber via 150 μm thick Kapton foil windows. A microwave electron cyclotron resonance plasma source (Ø 25 mm, described in detail in Ref. [12]) provided Ar ions for sample erosion. It was mounted at a distance of 8 cm from the sample and the grazing angle of incidence was set to 55° with respect to the sample surface.

In order to characterize the ion erosion process, a set of diffuse scatter patterns (scattering diagrams) has been recorded with a CCD camera (1024 × 256 pixels, pixel size 19 μm × 19 μm, integration time 5 s) that was placed at a distance of 1 m from the sample. The camera was cooled with liquid nitrogen to reduce the thermal noise. A beamstop was installed in front of the CCD camera to block the specular reflected beam and prevent detector overexposure. The X-ray energy was set to 17.5 keV (λ = 0.071 nm), and the grazing angle of the probe beam was 0.09°, which is just below the critical angle for total external reflection. The vertical X-ray beam size was set to 0.2 mm, while the horizontal beam size was set to 4.6 mm to favor a high intensity at the detector. As the scattering diagram is very narrow in the azimuthal (horizontal) plane, the scattered intensity was integrated in this direction through pixel binning.

The scattering diagram $\Pi(\theta)$ from an isotropic surface is, according to first order perturbation theory, proportional to the one-dimensional power spectral density (PSD_{1D}) function of the surface roughness (see, e.g., Ref. [13]). Therefore, the PSD-function can be deduced from the experimental data directly via:

$$\Pi(\theta) = \frac{1}{W_i}\frac{dW_{scat}}{d\theta} = \frac{k^3\left|(1-\varepsilon)T(\theta_0)T(\theta)\right|^2}{16\pi\,\sin\theta_0}\cdot \mathrm{PSD}_{1D}(\nu), \qquad (1)$$

with

$$\mathrm{PSD}_{1D}(\nu) = 4\int \left\langle z(\vec{\rho})z(0)\right\rangle \cos(2\pi\nu\rho)d\rho;$$

$$\nu = \frac{1}{\lambda}|\cos\theta - \cos\theta_0|; \quad T(\theta) = \frac{2\sin\theta}{\sin\theta + \sqrt{\varepsilon - \cos^2\theta}},$$

where W_i and dW_{scat} are the radiation powers of the incoming beam impinging under an angle θ_0 and of the outgoing beam scattered in the θ direction within an angular interval $d\theta$, respectively. The spatial frequency is denoted by ν; the dielectric constant of the sample by ε; the wavenumber by $k = 2\pi/\lambda$, and the amplitude transmittance of a perfectly smooth surface by $T(\theta)$. The function $z(\vec{\rho})$ describes the surface relief, and angular brackets denote an ensemble averaging. The procedure for normalization of the scattering data is described, e.g., in Ref. [14].

Table 1
Overview of the sample coding and properties.

Sample code	Ion energy (eV)	Preliminary roughening	Etch rate (nm/s)
NR_{1000}	1000	No	3.5
R_{1000}	1000	Yes	3.5
R_{300}	300	Yes	0.12

In addition to the scattering measurements, experiments were performed on etching of 60 nm thick Si films deposited onto Si substrates in order to establish the etch rate as a function of the ion energy. The film thickness before and after a short etching step was determined from a θ–2θ scan that was measured with a scintillator detector. The thus obtained etch rate was 0.12 nm/s at an ion energy of 300 eV and 3.5 nm/s at 1000 eV (argon pressure 1×10^{-3} mbar).

In two of the three experiments presented below, the sample surface was roughened beforehand with a 10 min, 1000 eV Ar^+ treatment at a grazing angle of $\theta = 10°$ and an Ar pressure of 1×10^{-3} mbar. Table 1 gives an overview of the samples used for the investigation reported in this paper.

3. Results and discussion

Figs. 1 and 2 show the evolution of the PSD-function and the rms roughness of the three samples studied. Sample NR_{1000} is initially very smooth with a rms roughness of only 0.15 nm in the $[2 \times 10^{-4}, 2 \times 10^{-2}\ \mathrm{nm}^{-1}]$ spatial frequency range. Nevertheless, no significant increase in roughness is observed during etching with 1000 eV Ar^+ ions despite the large removed thickness of 1.2 μm. In contrary, when the sample is roughened prior to the experiment (sample R_{1000}), very fast smoothening of the surface occurs during the first 20 s of the ion treatment. The roughness reduction is especially pronounced in the mid and high spatial frequency range, while the low frequency part of the roughness spectrum is much less affected.

The rms roughness of both samples (NR_{1000} and R_{1000}) becomes almost the same after about 20 s of etching, which demonstrates that the memory of the initial roughness is only lost after removal of 70 nm Si, despite the very small initial roughness of the samples (0.15 and 0.28 nm).

The PSD-function and the rms roughness of a beforehand roughened sample evolve more gradually when the etching energy is reduced to 300 eV (sample R_{300}), as can be expected from the 30-fold reduction of the etching rate. The high frequency roughness is reduced in the first 30 s of the etching treatment, after which it remains almost constant. At lower spatial frequencies, on the other hand, the initial smoothening is followed by a slower, but pronounced roughening.

In general, and compatible with recent results for flat Si targets at normal incidence and in a similar energy range [15], we obtain no pattern formation in our etching experiments. However, while for the non-roughened sample the ensuing surface morphology remains basically featureless as in [15], both samples R_{1000} and R_{300} develop non-trivial correlations at small length-scales/high spatial frequencies with increasing irradiation time (see Fig. 1), that can be described within the framework of surface kinetic roughening. This requires that the 1D PSD-function of the film roughness behaves as an inverse power law $\mathrm{PSD}_{1D}(\nu) \sim 1/\nu^{1+2\alpha}$ at high spatial frequencies ν. Hence, through analysis of the asymptotic behaviour of the PSD-function at large ν, one can determine the so-called static scaling exponent α. This exponent characterizes the saturated roughness and is found to equal $\alpha = 0.23 \pm 0.08$ for sample R_{1000} and

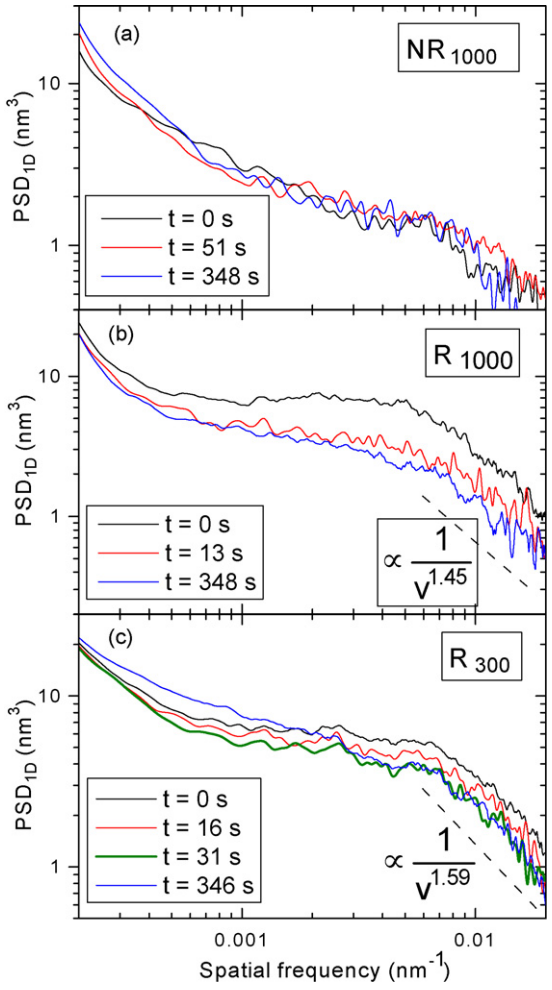

Fig. 1. Evolution of the PSD-function of the samples studied upon etching. The dashed lines indicate the asymptotic behavior for the PSD_{1D} at high spatial frequencies.

$\alpha = 0.30 \pm 0.05$ for sample R_{300}. Therefore, within the experimental error we can conclude that the value of α is independent of the ion energy. For sample NR_{1000} the exponent α is not clearly defined in the spatial frequency range measured in the XRS experiment.

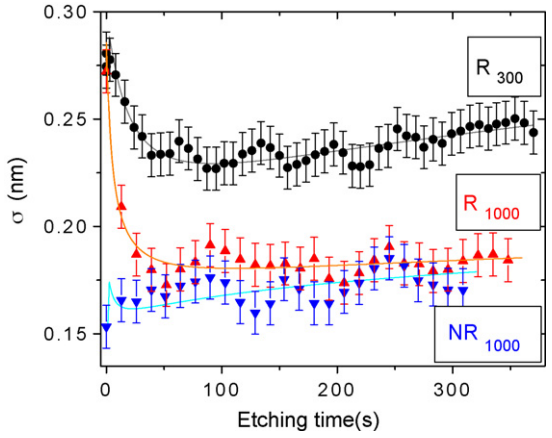

Fig. 2. The evolution of the root-mean-square roughness σ upon etching, for each of the three samples. The thick, solid lines represent the best fits in the framework of the Majaniemi model (2), (4). The curves R_{1000} and NR_{1000} have been fitted simultaneously with the same values for the fitting parameters. The, initially dominant, contribution of σ_E gives rise to a sharp increase of σ, and is followed by smoothening due to the decreasing value of σ_S.

The dynamic exponent β can be found from analysis of the rms roughness evolution with the erosion time $\sigma^2(t) = \int \mathrm{PSD}_{1D}(\nu)\, d\nu \sim t^{2\beta}$. However, this equation implies a perfectly smooth initial surface. In reality, the surface roughness upon etching is determined by two factors: the initial roughness of the initial substrate σ_S disappearing with the erosion time, and the etching induced roughness σ_E following the scaling law $\sigma_E(t) \sim t^{\beta}$.

The question how to distinguish between the contributions of σ_S and σ_E was considered in detail by Majaniemi et al. in Ref. [16], where the analysis was based on the linear theory of film growth or erosion. The authors of [16] demonstrated that it is necessary to discriminate two cases, depending on whether the correlation length of the treatment-induced roughening process $\zeta(t) \sim t^{\beta/\alpha}$ is smaller or larger than that associated with the initial roughness ζ_S. In the early stage of growth/erosion, the initial substrate roughness σ_S was found to give a constant contribution to the treated surface roughness $\sigma(t)$, regardless of the growth/erosion time:

$$\sigma^2(t) = \sigma_S^2 + \sigma_E^2(t); \quad \sigma_E = A \cdot t^{\beta}; \quad \zeta(t) \ll \zeta_S, \tag{2}$$

with A a proportionality constant.

However, when the correlation length of the treatment-induced roughness becomes larger than that of the initial substrate roughness, the contribution of the initial substrate to the surface evolution depends on the treatment time, i.e. $\sigma_S \to \sigma_S(t)$ in Eq. (2), and decays universally with the deposition/erosion time as

$$\sigma_S(t) = \sigma_S(0) \cdot \zeta_S/\zeta(t); \quad \zeta(t) \gg \zeta_S. \tag{3}$$

To obtain a smooth transition between the two limiting cases (2) and (3), the authors of [12] suggest the following formula

$$\sigma_S(t) = \frac{\sigma_S(0)}{(1 + t/t_S)^{\beta/\alpha}}, \tag{4}$$

where t_S is a fitting parameter.

The solid curves in Fig. 2 are the result of fitting $\sigma^2(t)$ according to Eqs. (2) and (4), using α as obtained from the asymptote in Fig. 1, and taking the 5 s recording time of the CCD detector into account. Note that evolution of the rms roughness of samples NR_{1000} and R_{1000} is described properly with the use of the same set of fitting parameters, namely, $\beta = 0.07 \pm 0.01$ and $t_s = 2.6 \pm 0.4$ s. As seen in Fig. 2, the Majaniemi model (Eqs. (2) and (4)) simultaneously explains smoothening as well as roughening of a surface upon ion erosion, depending on the rms roughness of the initial substrate. Note that the very small value of β could also be compatible with very slow logarithmic growth of the roughness. Similarly, the evolution of the rms roughness of the sample R_{300} is well described by Eqs. (2), (4), although the fitting parameters are different: $\beta = 0.14 \pm 0.02$ and $t_s = 16 \pm 2$ s, demonstrating that the value of the dynamic scaling exponent β depends on the ion energy.

The derived sets of scaling exponents α and β correspond to none of the growth/erosion equations reported in the literature. Such a disagreement has already been pointed out in literature (see, e.g., Ref. [17] and references therein) and may be due to the high degree of complexity of the eroded surface dynamics.

4. Conclusions and outlook

We analyzed the roughness evolution of Si substrates upon Ar ion etching. The evolution was demonstrated to depend on the initial substrate roughness σ_S: a small increase of the rms roughness was observed for the smoothest sample upon etching at an ion energy of 1000 eV, while very fast smoothening was observed during the first 30 s of etching of a rougher sample. After 30 s of ion erosion, the surface dynamics were the same for both samples, regardless of the initial surface roughness. Smoothening was also observed for an ini-

tially rough sample that was eroded at a lower ion energy (300 eV).

The static scaling exponent was demonstrated to be independent of the ion energy (within experimental uncertainty): $\alpha = 0.23 \pm 0.08$ for etching at 1000 eV, and $\alpha = 0.30 \pm 0.05$ for etching at 300 eV. The Majaniemi model, which divides the eroded surface roughness into contributions of the initial substrate roughness and the erosion induced roughness, was demonstrated to properly describe our experimental data. This model, based on the analysis of linear equations describing growth/erosion processes, was used to fit our data and obtain the dynamic scaling exponent β. Using the same set of parameters, the model explains both the observed roughening of the smoothest sample and the smoothening of the roughened sample upon erosion with 1000 eV Ar^+. While no ion energy dependency was found for the static scaling exponent, the dynamic scaling exponent proved to increase with decreasing ion energy: $\beta = 0.07 \pm 0.01$ at $E = 1000$ eV and $\beta = 0.14 \pm 0.02$ at $E = 300$ eV. The scaling exponents α and β are important parameters for the determination of a comprehensive theory of ion erosion of (Si) surfaces. However, in order to accomplish the greater goal of a full theory of ion erosion of Si surfaces, it is necessary to investigate a larger part of the parameter space. More experiments have to be conducted in which the ion energy, angle of incidence, ion mass, and initial surface roughness are varied. The comprehensive theory resulting from such experiments would be a leap forward in the understanding of ion-solid interactions, and be of great interest for miscellaneous thin film applications.

Acknowledgements

I.V. Kozhevnikov acknowledges the support of the ISTC (project #3124). V.I.T.A. de Rooij-Lohmann, F. Bijkerk, and A.E. Yakshin acknowledge the FOM Industrial Partnership Programme I10 ('XMO') which is carried out under contract with Carl Zeiss SMT AG, Oberkochen, and the 'Stichting voor Fundamenteel Onderzoek der Materie (FOM)', Utrecht, the latter being financially supported by the 'Nederlandse Organisatie voor Wetenschappelijk Onderzoek (NWO)'. R. Cuerno acknowledges partial support by grants FIS2006-12253-C06-01 (MEC, Spain), FIS2009-12964-C05-01, (MICINN, Spain), and CCG08-CSIC/MAT-3457 (CAM, Spain). The authors further acknowledge the European Synchrotron Radiation Facility, Grenoble, for providing the measurement facilities (beamline BM05).

References

[1] A. Schindler, T. Haensel, A. Nickel, H.-J. Thomas, H. Lammert, F. Siewert, Optical Manufacturing and Testing V, SPIE, San Diego, CA, USA, 2004, p. 64.
[2] F. Frost, R. Fechner, B. Ziberi, D. Flamm, A. Schindler, Thin Solid Films 459 (1–2) (2004) 100.
[3] J. Verhoeven, L. Chunguang, E.J. Puik, M.J. van der Wiel, T.P. Huijgen, Applied Surface Science 55 (2–3) (1992) 97.
[4] R. Schlatmann, C. Lu, J. Verhoeven, E.J. Puik, M.J. van der Wiel, Applied Surface Science 78 (2) (1994) 147.
[5] E. Louis, H.J. Voorma, N.B. Koster, L. Shmaenok, F. Bijkerk, R. Schlatmann, J. Verhoeven, Y.Y. Platonov, G.E. van Dorssen, H.A. Padmore, Microelectronic Engineering 23 (1–4) (1994) 215.
[6] R. Cuerno, L. Vázquez, R. Gago, M. Castro, Journal of Physics: Condensed Matter 21 (2009) 220301.
[7] A.-L. Barabási, H.E. Stanley, Fractal Concepts in Surface Growth, Cambridge University Press, Cambridge, 1995.
[8] F. Family, T. Vicsek, Journal of Physics A: Mathematical and General 18 (2) (1985) L75.
[9] L. Peverini, E. Ziegler, I. Kozhevnikov, Applied Physics Letters 91 (5) (2007) 053121.
[10] R. Cuerno, A.-L. Barabási, Physical Review Letters 74 (23) (1995) 4746.
[11] L. Peverini, E. Ziegler, T. Bigault, I. Kozhevnikov, Physical Review B 72 (4) (2005) 045445.
[12] R. Anton, T. Wiegner, W. Naumann, M. Liebmann, C. Klein, C. Bradley, The 8th International Conference on Ion Sources, AIP, Kyoto (Japan), 2000, p. 1177.
[13] V.E. Asadchikov, I.V. Kozhevnikov, Y.S. Krivonosov, R. Mercier, T.H. Metzger, C. Morawe, E. Ziegler, Nuclear Instruments and Methods in Physics Research A 530 (3) (2004) 575.
[14] L. Peverini, I. Kozhevnikov, E. Ziegler, Physica Status Solidi (a) 204 (8) (2007) 2785.
[15] C.S. Madi, B. Davidovitch, H.B. George, S.A. Norris, M.P. Brenner, M.J. Aziz, Physical Review Letters 101 (24) (2008) 246102.
[16] S. Majaniemi, T. Ala-Nissila, J. Krug, Physical Review B 53 (12) (1996) 8071.
[17] L. Peverini, E. Ziegler, T. Bigault, I. Kozhevnikov, Physical Review B (Condensed Matter and Materials Physics) 76 (4) (2007) 045411.